Journal of Materials Chemistry C

PAPER

View Article Online
View Journal

Cite this: DOI: 10.1039/c5tc00276a

Highly conductive PEDOT:PSS films by post-treatment with dimethyl sulfoxide for ITO-free liquid crystal display

Tsu-Ruey Chou,[a] Szu-Hua Chen,[a] Yen-Te Chiang,[b] Yi-Ting Lin[a] and Chih-Yu Chao*[abc]

Received 28th January 2015,
Accepted 25th February 2015

DOI: 10.1039/c5tc00276a

www.rsc.org/MaterialsC

In this study, a simple and effective method to enhance the conductivity of poly(3,4-ethylenedioxythiophene):poly(styrenesulfonate) (PEDOT:PSS) thin films from 0.7 to 1185 S cm^{-1} by post-treatment with dimethyl sulfoxide (DMSO) is demonstrated. After the rubbing technique was applied, the DMSO-treated PEDOT:PSS film could be used as both the transparent electrode and the alignment layer to fabricate ITO-free liquid crystal (LC) cells. The electro-optical properties of LC cells fabricated by the rubbed PEDOT:PSS were comparable to those constructed by ITO and polyimide. This work indicates that the highly conductive PEDOT:PSS film is a promising material for ITO-free LC devices.

Introduction

Optoelectronic devices such as liquid crystal displays (LCDs), organic photovoltaics (OPVs) and organic light-emitting diodes (OLEDs) have received great interest these years due to their mechanical flexibility, light weight, and prospective potential for roll-to-roll manufacturing. Among these devices, LCD has been commercialized since at least 30 years and has become the most widely used display in our daily life. Recently, researchers have developed several new modes of liquid crystal (LC) devices to achieve high performance display, *e.g.*, in-plane switching,[1] patterned vertical alignment,[2] and fringe-field switching.[3] No matter in which modes, LC devices act as a light valve to control the transmission of backlight. Therefore, the transparent electrode is required for LC device architecture, even in the case of reflective LCDs.

Indium tin oxide (ITO), which could be deposited on both glass and plastic substrates, has been the most commonly used material as the transparent electrode for decades. However, the limited indium on earth and the fragile characteristic of ITO thin films increase the cost of LCDs and restrict the applicability of ITO on flexible electronic devices, respectively.[4–6] Furthermore, the total reflection at the glass/ITO interface,[7] poor transparency in the blue spectrum,[8] and poor adhesion to organic materials degrade the performance of optoelectronic devices which use ITO as the transparent electrode. These drawbacks make ITO a non-ideal material in the future, and thus searching for an alternative to replace ITO is an unavoidable task.

To date, many materials such as carbon nanotube,[9–12] metal nanowires,[13,14] thin metal,[15] graphene,[16,17] and conducting polymers[18–20] have been investigated as alternatives to replace ITO. In particular, poly(3,4-ethylenedioxythiophene):poly-(styrenesulfonate) (PEDOT:PSS) is one of the most potential materials due to its excellent mechanical flexibility, good thermal stability, and high transparency in the visible range. It can be dispersed in water and several organic solvents and hence PEDOT:PSS films could be prepared by simple solution processes such as spin coating or inject printing.[21–23] However, the conductivity of the pristine PEDOT:PSS film, typically below 1 S cm^{-1}, is extremely lower than that of the commercialized ITO, which makes it inappropriate for practical applications. The insulating PSS, which makes the conductive PEDOT to be easily dispersed in water, is the main reason for the low conductivity of PEDOT:PSS films. In order to improve the conductivity of PEDOT:PSS, several methods have been reported, including doping additional organic compounds with their boiling points higher than the boiling point of water, such as dimethyl sulfoxide (DMSO),[24] ionic liquid,[25] dimethyl sulfate,[26] or polyol,[27] into PEDOT:PSS aqueous solution and processing post-treatment of PEDOT:PSS films with cosolvents,[28] ethylene (EG),[29] salt,[30] or inorganic acid.[31] Generally speaking, doping polar solvents into PEDOT:PSS leads to morphology changes including extended grain size and better interconnection between PEDOT chains, whereas post-treatment usually results in both morphology changes and removal of unwanted PSS on the film surface. Therefore, methods including

[a] Department of Physics, National Taiwan University, No. 1, Sec. 4, Roosevelt Rd., Taipei 10617, Taiwan. E-mail: cychao@phys.ntu.edu.tw
[b] Institute of Applied Physics, National Taiwan University, No. 1, Sec. 4, Roosevelt Rd., Taipei 10617, Taiwan
[c] Molecular Imaging Centre, National Taiwan University, No. 1, Sec. 4, Roosevelt Rd., Taipei 10617, Taiwan

post-treatment usually show better results than those simply using additives to improve the conductivity of PEDOT:PSS films.

In this paper, the conductivity enhancement of highly conductive PEDOT:PSS films through post-treatment with DMSO was performed. The conductivity enhanced greatly by four orders of magnitude, which is attributed to the removal of PSS on the surface and the conformational change of the PEDOT:PSS film. After we implemented the rubbing technique with a polyester cloth, the DMSO-treated highly conductive PEDOT:PSS films revealed uniform planar alignment which could be used as the alignment layer in the LC device. The measured electro-optical properties show comparable characteristics relative to those of LC cells assembled by the polyimide (PI) coated ITO glass. Here our work shows the potential and facility of highly conductive PEDOT:PSS films that can be used as both the transparent electrode and the alignment layer in LC devices for ITO-free LC displays.

Experimental

The PEDOT:PSS aqueous solution (Clevios PH1000) was purchased from Heraeus Clevios GmbH with a solid concentration 1.0–1.3 wt% and the weight ratio of PEDOT to PSS was 0.4. DMSO (99.9%, anhydrous) was purchased from Sigma-Aldrich with a water content less than 0.005 wt%. All the materials were used without further purification. The chemical structures of these materials are shown in Scheme 1.

Glass substrates (2.5 × 2.5 cm^2) were cleaned with detergent, acetone, isopropyl alcohol and deionised (DI) water successively. After drying in the oven, glass substrates were treated with air plasma for 4 min to enhance the wettability. A single-layer PEDOT:PSS thin film was deposited on a glass substrate *via* spin coating at 3000 rpm for 60 s and then annealed at 120 °C for 15 min. The PEDOT:PSS aqueous solution was filtered through a 0.45 μm syringe filter prior to spin coating. Next, a small amount of DMSO was dropped directly (hereafter referred as the 'drop' method) on the PEDOT:PSS film at 120 °C and dried for 15 min. The treated film was then rinsed with DI water several times to remove the excess PSS on the film and finally dried at 120 °C for 15 min again. Thicker PEDOT:PSS films were prepared by multiple coatings and treated in the same way described above on each PEDOT:PSS layer.

The sheet resistance (R_s) of PEDOT:PSS films was measured by the four point probe method and the electrical conductivity (σ) was calculated using the formula:

$$\sigma = 1/(R_s \times d) \quad (1)$$

where d is the film thickness. The surface morphology and the thickness of the PEDOT:PSS film were characterized and measured by means of an Park XE-100 atomic force microscope (AFM) operated in tapping mode. The resonance frequency of the tip (PPP-RT-NCHR, Nanosensors) we used in this study was 330 kHz. Raman spectra were measured using a Horiba Jobin Yvon HR800 confocal μ-Raman system. The wavelength and power of the excitation laser are 633 nm and 5.4 mW, respectively. Optical transmission and absorption spectra were taken using a UV-vis-NIR spectrometer (JASCO V-670).

The empty LC cells were fabricated using two glass substrates coated with double layers of highly conductive PEDOT:PSS films. The top layer was rubbed with a polyester cloth after post-treatment in order to yield a unidirectional planar alignment. Besides, empty LC cells constructed from ITO glass (sheet resistance 95 Ω □$^{-1}$) coated with a polyimide layer (AL-12G, Daily-Polymer) were made for comparison. The cell configuration of all samples is 90° twisted nematic (TN) mode with a 4 μm cell gap ensured by silica spacers. Thereafter, nematic LCs (DF-7538A, Daily-Polymer) were injected into empty cells by means of capillary action in the isotropic phase. The structures of LC cells fabricated using glass/PEDOT:PSS and glass/ITO/PI are shown in Fig. 1.

After sample preparation, polarizing optical microscopy (POM) was employed to examine the uniformity of the LC alignment. The voltage–transmittance (V–T) curve and response time of each cell from a He–Ne laser source were measured using a silicon photo detector. All cells were placed between a pair of cross-polarizers and measured by applying a square wave voltage with a frequency of 1 kHz in the normally white mode.

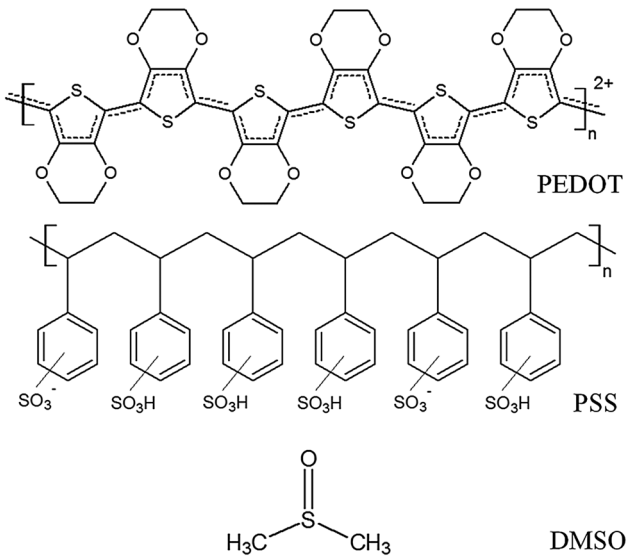

Scheme 1 Chemical structures of PEDOT, PSS, and DMSO.

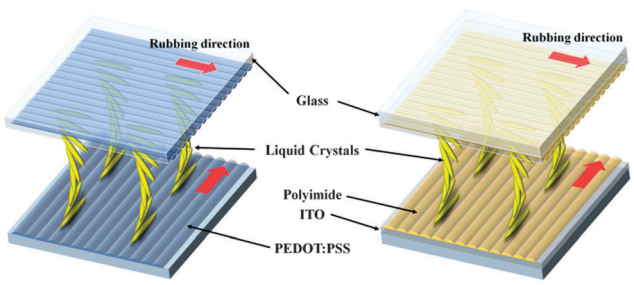

Fig. 1 The structure of LC cells fabricated using the rubbed highly conductive PEDOT:PSS on glass and polyimide on ITO glass.

Results and discussion

Previous reports have shown that adding a small amount of DMSO or other solvents into high conductive PH 1000 PEDOT:PSS could enhance the conductivity of the PEDOT:PSS film.[24] Besides, some studies showed conductivity enhancement upon immersing the dried PEDOT:PSS film into EG or treatment with polar solvent or cosolvents.[28,29,31] Therefore, we are interested in which method shows the best result using DMSO. Fig. 2 shows the conductivities along with the error bar of the pristine PEDOT:PSS and after three conductivity enhancing methods using anhydrous DMSO. The '5% DMSO' was done by mixing 5% (v/v) DMSO in the PEDOT:PSS aqueous solution and stirred for 24 h prior to spin coating. The 'dip' treatment was performed by immersing the annealed PEDOT:PSS film into DMSO at room temperature for 30 min and dried at 120 °C for 15 min. The drop method was done using the procedure mentioned in the experimental section. The average conductivity increased from 0.7 S cm^{-1} to 755, 789, 994 S cm^{-1} for samples with 5% DMSO, treated with the dip method, and treated with the drop method, respectively. Obviously, the drop method shows the best result compared with the others. Therefore, the drop method was adopted as the post-treatment process for the following experiments in this study.

Previously, Xia and Ouyang demonstrated that the conductivity of PEDOT:PSS film could be enhanced by post-treatment with cosolvents including water, methanol, ethanol, 1,2-dichlorobenzene, *etc.* They carried out a study to find out whether anhydrous methanol or normal methanol (water less than 0.05%) is a better candidate to enhance the conductivity of the less conductive PEDOT:PSS (Clevios VP AI4083), which is often used as a buffer layer in OLED or OPV cells. Their results showed that the conductivity of the less conductive PEDOT:PSS film treated with normal methanol improved more than those treated with anhydrous methanol.[28] This indicates that even a small amount of water in the normal methanol could influence the result of post-treatment. Motivated by this study, we added a small amount of DI water into the anhydrous DMSO. In our experiments, the concentration of DI water varied from 0 to 6% (v/v). Fig. 3 shows the variation of the conductivity of PEDOT:PSS films treated with DMSO doped with different concentrations of DI water.

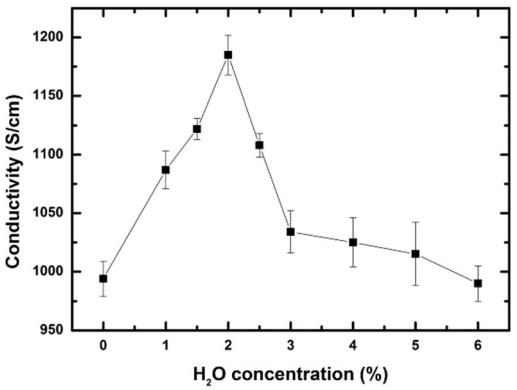

Fig. 3 Variation of the conductivity of PEDOT:PSS films treated with DMSO doped with different concentrations of DI water.

The highest conductivity (1185 S cm^{-1}) was obtained when the doping concentration was 2%. The conductivity decreased gradually when the doping concentration was above 3%.

Various mechanisms have been proposed to explain the conductivity enhancement of PEDOT:PSS films. For those methods utilizing the post-treatment process, two mechanisms contribute to the conductivity enhancement mainly: the removal of those excess PSS on the surface of the PEDOT:PSS film and the conformational change of the PEDOT and PSS chain. The surface of the pristine PEDOT:PSS film contains more PSS than the bulk region.[32] Therefore, removing the hygroscopic and insulating PSS on the film surface is crucial to increase the stability and conductivity of PEDOT:PSS. Fig. 4 shows the UV absorption spectra of the pristine and the DMSO-treated PEDOT:PSS films. The two absorption peaks at 195 nm and 225 nm correspond to the aromatic rings of PSS.[33] From Fig. 4, it is clear that the intensity of these two bands decreased after DMSO post-treatment, which implies that the amount of PSS chains in the PEDOT:PSS film reduced after the post-treatment. Besides, after the DMSO post-treatment, the film thickness reduced from 60 nm to 40 nm, which is attributed to the removal of PSS chains.

The PEDOT and PSS form a core–shell structure in the pristine film where the core region is conductive PEDOT rich

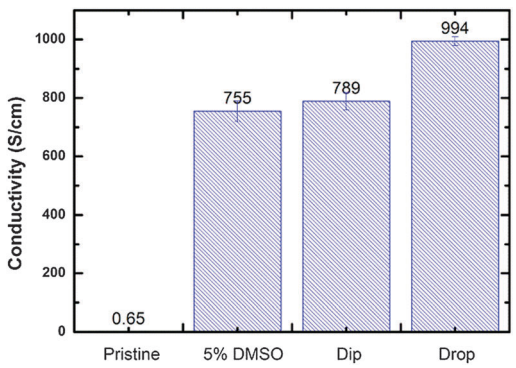

Fig. 2 Conductivities of PEDOT:PSS films treated with DMSO by different methods.

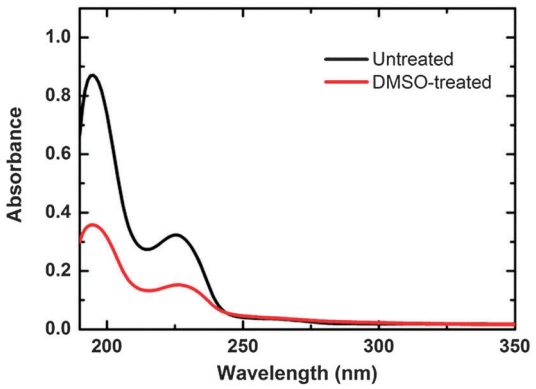

Fig. 4 UV absorption spectra of PEDOT:PSS films before and after the DMSO post-treatment.

and the shell region is insulating PSS rich.[34] Since the conductive core is surrounded by the insulating shell, it is hard for those carriers on the PEDOT chain to transport through the film, and thus the pristine film shows low conductivity. The surface topography and phase images of the PEDOT:PSS film before and after the DMSO post-treatment were captured by AFM, as shown in Fig. 5. From Fig. 5(a) and (b), it is clear that the PEDOT:PSS film turned from a core–shell structure to an entangled wire-like structure after the post-treatment. This conformational change is attributed to the DMSO post-treatment which reduces the Coulombic attraction between PEDOT and PSS. The reduced attraction results in phase separation between the hydrophobic PEDOT and hydrophilic PSS. Along with the removal of PSS, PEDOT chains turned from a coiled to a linear structure, as shown in Fig. 5(c) and (d). This conformational change reduces the energy barrier of charge hopping on the PEDOT:PSS film which contributes to the conductivity enhancement. The surface roughness (mean roughness) increased from 1.14 nm to 1.56 nm after the post-treatment, which is still acceptable smoothness. To further confirm the conformational change of PEDOT:PSS films after the DMSO post-treatment, Raman spectroscopy was performed. Fig. 6 shows the Raman spectra of the pristine and the DMSO-treated PEDOT:PSS films. The strongest band between 1400 and 1500 cm^{-1} corresponds to the $C_\alpha{=}C_\beta$ symmetric stretching of the five-membered thiophene ring on the PEDOT chains.[35,36] The peak value of this band is red shifted from 1427 to 1414 cm^{-1} after the post-treatment, which indicates that the resonant structure of the PEDOT chains changes from the benzoid structure to the quinoid structure.[35,37] The benzoid structure

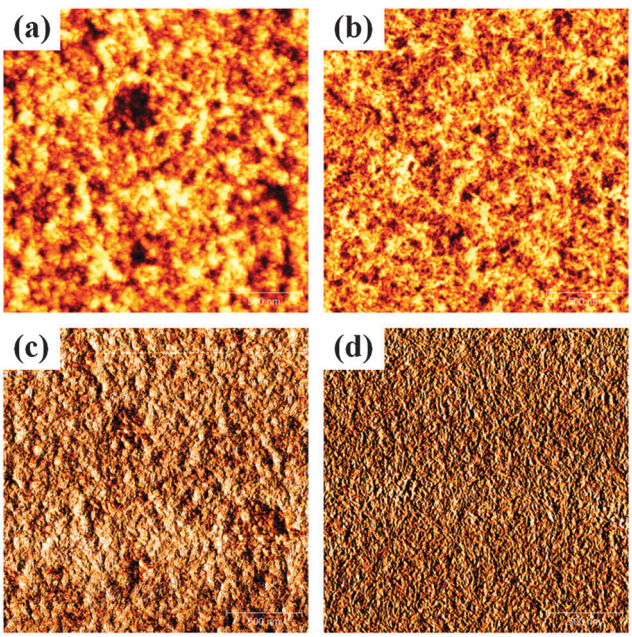

Fig. 5 AFM images of PEDOT:PSS films before (a and c) and after (b and d) the DMSO post-treatment. (a) and (b) are surface topography images while (c) and (d) are phase images. The dimension of these images is 2 μm × 2 μm.

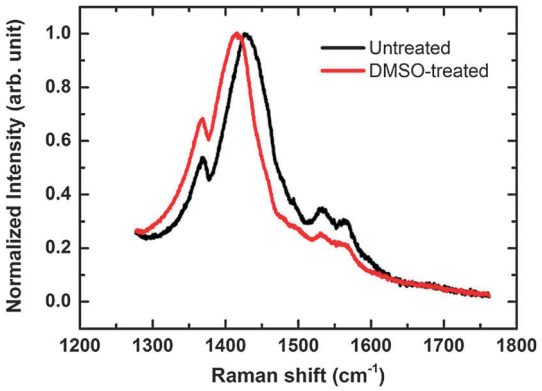

Fig. 6 Raman spectra of PEDOT:PSS films before and after the DMSO post-treatment.

is the favoured structure for the coil conformation while the quinoid structure is the favoured structure for the expanded-coil or the linear conformation.[38] Therefore, the measured red shift in Raman spectra confirms the conformational change of the PEDOT chains after we performed the DMSO post-treatment.

In order to reduce the sheet resistance of the PEDOT:PSS film, multilayer architecture was obtained. This can be obtained by spin coating the PEDOT:PSS solution multiple times. The post-treatment was carried out on each layer with 2% DI water doped DMSO. The sheet resistance reduced from 211 to 103 and 67 Ω $\square^{-1}$ for single layer, double layers and triple layers, respectively. The conductivity of the third layer is slightly lower, which is similar to the result of other groups.[31] The sheet resistances of the multilayer film are comparable to or lower than that of the ITO substrate used for LC devices, which has a typical value of about 100 Ω $\square^{-1}$. On the other hand, Fig. 7 presents the transmittance spectra of ITO and DMSO treated PEDOT:PSS films with different layers. The transmittance measured in this study excludes the absorption of the glass substrate since the glass substrates we used for PEDOT:PSS coating were different from those employed for commercial ITO deposition. The transmittance at 550 nm is 96%, 93% and 89% for single layer, double layers and triple layers, respectively. This result indicates that the thick film results in transmission loss.

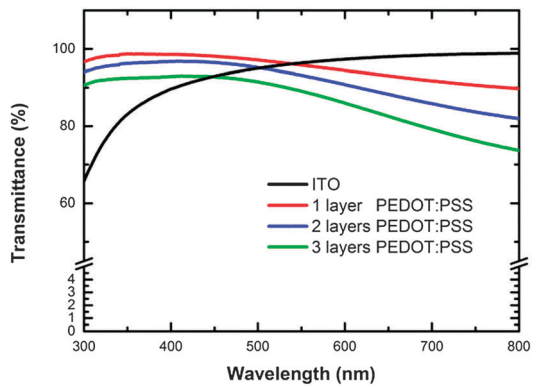

Fig. 7 Transmittance spectra of ITO and PEDOT:PSS film with different layers. The sheet resistance of the ITO is 95 Ω $\square^{-1}$.

The sheet resistance and transmittance of the double layer sample are comparable to those of the ITO (transmittance 96% and sheet resistance 95 Ω $\square^{-1}$) we used for comparison in this study.

In order to align LC molecules on the PEDOT:PSS film, the rubbing process was employed. Several materials such as velvet cloth and silicon rubber sheet have been adopted in the rubbing process. In our case, we used a polyester cloth to generate the oriented nanoscale-groove structure on the surface of the PEDOT:PSS layer. The surface relief structures of the rubbed PEDOT:PSS films captured by AFM are shown in Fig. 8. The orientation of induced grooves is uniformly aligned along the rubbing direction and the depth of the grooves ranges from a few nanometers to 10 nm. Previous studies have shown that the surface topography of the substrate and the chemical reaction between LC molecules and the alignment layer play crucial roles in the alignment mechanism.[39,40] In this study, we consider that it is the grooved surface of the PEDOT:PSS film and the aromatic rings of PSS which account for the LC alignment.

Fig. 9(a) and (b) show POM images of LC cells fabricated using the rubbed highly conductive PEDOT:PSS films with and without the applied external field, respectively. These images were taken in normally black mode. In normally black mode, it would be easy to observe light leakage spots if the TN configuration achieved by the rubbed PEDOT:PSS films has some defects. In these pictures, uniform dark and bright states were obtained which indicates that the rubbed highly conductive PEDOT:PSS films could align LC molecules well and it would not generate optically observable flaws in the bright state.

In order to investigate the electro-optical properties of the LC cells using the rubbed highly conductive PEDOT:PSS as both the electrode and alignment layer, *V–T* characteristics and response times of these samples were measured. Fig. 10 shows the normalized transmittance of TN LC cells fabricated using glass/PEDOT:PSS and glass/ITO/PI under applied AC square wave voltage with the amplitude varying from 0 to 4 V. Measured results indicate that the *V–T* characteristics of cells constructed by PEDOT:PSS were similar to those of the samples fabricated by PI coated ITO glass. In comparison with the *V–T* curve of the sample using ITO and PI, the *V–T* curve of the sample using

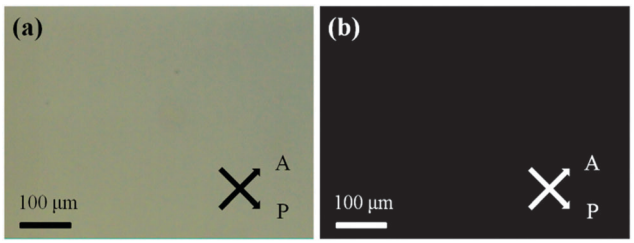

Fig. 9 POM images of TN LC cells fabricated by the rubbed highly conductive PEDOT:PSS films in normally black mode (a) with and (b) without the applied external field.

PEDOT:PSS shifts to higher voltage slightly. This is due to the difference in conductivity between PEDOT:PSS and ITO, which leads to a slight voltage drop on the PEDOT:PSS electrode. The threshold voltage and driving voltage are defined as the voltage corresponding to 90% and 10% of the initial transmittance, respectively. The measured threshold and driving voltage of the sample using PEDOT:PSS were 1.65 V and 2.67 V, which were very close to the results of the sample fabricated by ITO and PI (1.55 V and 2.55 V).

Fig. 11 shows the response time characteristics of TN LC cells fabricated using glass/PEDOT:PSS and glass/ITO/PI under applied AC square wave voltage with an amplitude of 6 V. Rise time and decay time are defined as the time interval between 90% and 10% of the initial transmittance after the external voltage was applied and removed, respectively. Response time is defined as the sum of rise time and decay time. The measured rise time and decay time of the samples fabricated using PEDOT:PSS were 3.36 ms and 15.57 ms respectively, which were faster than those of the samples using ITO and PI (4.02 ms and 25.49 ms). The LC cell constructed by PEDOT:PSS shows a faster response time, especially in the decay time. One reason accounting for this phenomenon might be the lack of the PI layer. When the applied voltage was removed, some induced dipole moments in the PI layer generated by the external electric field increase the time for LC molecules to rotate back to the twist state. To sum up, threshold voltage and

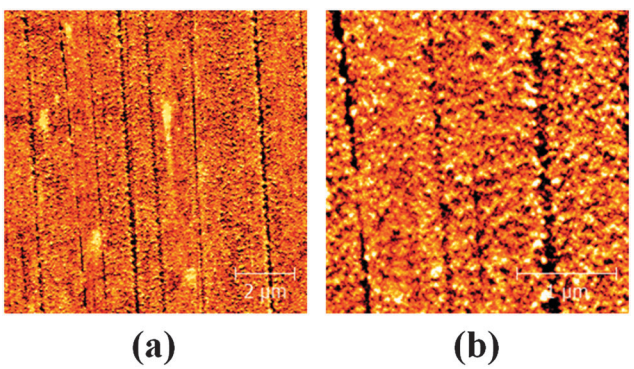

Fig. 8 Surface topography of the rubbed highly conductive PEDOT:PSS films. The dimensions of these images are (a) 10 μm × 10 μm and (b) 3 μm × 3 μm.

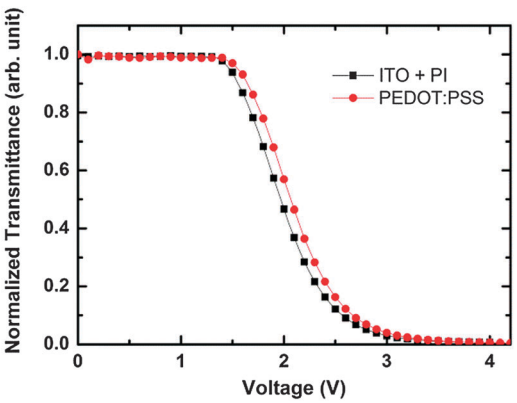

Fig. 10 Transmittance of TN LC cells fabricated by the rubbed highly conductive PEDOT:PSS on glass and polyimide on ITO glass under applied AC square wave voltage.

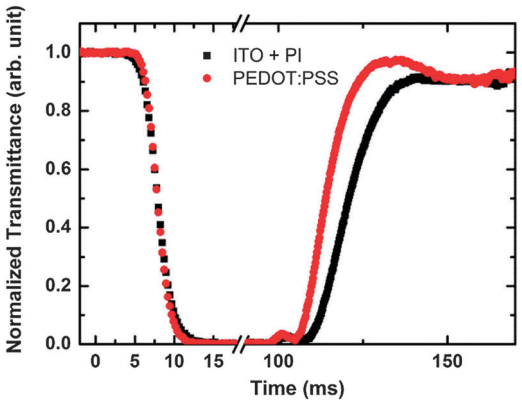

Fig. 11 Response time characteristics of TN LC cells fabricated by the rubbed highly conductive PEDOT:PSS on glass and polyimide on ITO glass.

response time are key factors which correspond to the power consumption and the image quality of LC devices in the LCD industry, respectively. The measured results show that PEDOT:PSS used as both a transparent electrode and an alignment layer in LC cells possesses low power consumption and fast response characteristics as traditional LC devices and could further expand LC devices to the flexible electronic field.

Conclusion

In summary, a simple and effective method to enhance the conductivity of PEDOT:PSS thin films by four orders of magnitude is demonstrated. The conductivity of the pristine PEDOT:PSS film increased drastically from 0.7 to 1185 S cm^{-1} after post-treatment with 2% of DI water doped DMSO. The removal of the insulating PSS together with the re-ordering and conformation changes of the PEDOT and PSS chains are the prime reasons for the conductivity enhancement observed in this study. Uniform LC alignment on the highly conductive PEDOT:PSS film was achieved by using the rubbing technique. The electro-optical properties of TN LC cells fabricated by the rubbed highly conductive PEDOT:PSS film show comparable results relative to those fabricated by ITO and PI. This work indicates that the highly conductive PEDOT:PSS film is a promising material as both the transparent electrode and the alignment layer to replace ITO for ITO-free and flexible LC displays.

Acknowledgements

One of us (C.Y.C.) acknowledges the support from National Taiwan University, Ministry of Science and Technology, and Ministry of Education of the Republic of China. The authors would like to thank Mr Yen-Cheng Chao for his helpful assistance in AFM measurements.

Notes and references

1 M. Ohe and K. Kondo, *Appl. Phys. Lett.*, 1995, **67**(26), 3895.
2 Y.-J. Lee, Y.-K. Kim, S. I. Jo, J. S. Gwag, C.-J. Yu and J.-H. Kim, *Opt. Express*, 2009, **17**(12), 10298.
3 S. H. Lee, S. L. Lee and H. Y. Kim, *Appl. Phys. Lett.*, 1998, **73**(20), 2881.
4 D. R. Cairns, R. P. Witte, D. K. Sparacin, S. M. Sachsman, D. C. Paine, G. P. Crawford and R. R. Newton, *Appl. Phys. Lett.*, 2000, **76**(11), 1425.
5 C. S. Tao, J. Jiang and M. Tao, *Sol. Energy Mater. Sol. Cells*, 2011, **95**, 3176.
6 A. Chipman, *Nature*, 2007, **449**, 131.
7 K. Saxena, V. K. Jain and D. S. Mehta, *Opt. Mater.*, 2009, **32**, 221.
8 J. M. Phillips, R. J. Cava, G. A. Thomas, S. A. Carter, J. Kwo, T. Siegrist, J. J. Krajewski, J. H. Marshall, W. F. Peck and D. H. Rapkine, *Appl. Phys. Lett.*, 1995, **67**(15), 2246.
9 Z. C. Wu, Z. H. Chen, X. Du, J. M. Logan, J. Sippel, M. Nikolou, K. Kamaras, J. R. Reynolds, D. B. Tanner, A. F. Hebard and A. G. Rinzler, *Science*, 2004, **305**, 1273.
10 M. Zhang, S. L. Fang, A. A. Zakhidov, S. B. Lee, A. E. Aliev, C. D. Williams, K. R. Atkinson and R. H. Baughman, *Science*, 2005, **309**, 1215.
11 G. Gruner, *J. Mater. Chem.*, 2006, **16**, 3533.
12 P. Joshi, L. F. Zhang, Q. L. Chen, D. Galipeau, H. Fong and Q. Q. Qiao, *ACS Appl. Mater. Interfaces*, 2010, **2**(12), 3572.
13 J.-Y. Lee, S. T. Connor, Y. Cui and P. Peumans, *Nano Lett.*, 2008, **8**(2), 689.
14 P.-C. Hsu, S. Wang, H. Wu, V. K. Narasimhan, D. S. Kong, H. R. Lee and Y. Cui, *Nat. Commun.*, 2013, **4**, 2522.
15 J. Meiss, M. K. Riede and K. Leo, *Appl. Phys. Lett.*, 2009, **94**, 013303.
16 V. C. Tung, L.-M. Chen, M. J. Allen, J. K. Wassei, K. Nelson, R. B. Kaner and Y. Yang, *Nano Lett.*, 2009, **9**(5), 194.
17 X. G. Mei and J. Y. Ouyang, *Carbon*, 2011, **49**, 5389.
18 Y. J. Xia, K. Sun and J. Y. Ouyang, *Energy Environ. Sci.*, 2012, **5**, 5325.
19 J. E. Yoo, K. S. Lee, A. Garcia, J. Tarver, E. D. Gomez, K. Baldwin, Y. M. Sun, H. Meng, T.-Q. Nguyen and Y.-L. Loo, *Proc. Natl. Acad. Sci. U. S. A.*, 2010, **107**(13), 5712.
20 S.-I. Na, S.-S. Kim, J. Jo and D.-Y. Kim, *Adv. Mater.*, 2008, **20**, 4061.
21 L. B. Groenendaal, F. Jonas, D. Freitag, H. Pielartzik and J. R. Reynolds, *Adv. Mater.*, 2000, **12**(7), 481.
22 Y. Cao, G. Yu, C. Zhang, R. Menon and A. J. Heeger, *Synth. Met.*, 1997, **87**, 171.
23 S. Kirchmeyer and K. Reuter, *J. Mater. Chem.*, 2005, **15**, 2077.
24 A. Laskarakis, P. G. Karagiannidis, D. Georgiou, D. M. Nikolaidou and S. Logothetidis, *Thin Solid Films*, 2013, **541**, 102.
25 C. Badre, L. Marquant, A. M. Alsayed and L. A. Hough, *Adv. Funct. Mater.*, 2012, **22**, 2723.
26 M. Reyes-Reyes, I. Cruz-Cruz and R. Lopez-Sandoval, *J. Phys. Chem. C*, 2010, **114**, 20220.
27 J. S. Huang, P. F Miller, J. S. Wilson, A. J. de Mello, J. C. de Mello and D. D. C. Bradley, *Adv. Funct. Mater.*, 2005, **15**(2), 290.
28 K. Sun, Y. J. Xia and J. Y. Ouyang, *Sol. Energy Mater. Sol. Cells*, 2012, **97**, 89.
29 Y. H. Kim, C. Sachse, M. L. Machala, C. May, L. Muller-Meskamp and K. Leo, *Adv. Funct. Mater.*, 2011, **21**, 1076.

30 Y. J. Xia and J. Y. Ouyang, *Org. Electron.*, 2010, **11**, 1129.
31 Y. J. Xia, K. Sun and J. Y. Ouyang, *Adv. Mater.*, 2012, **24**, 2436.
32 S.-I. Na, G. Wang, S.-S. Kim, T.-W. Kim, S.-H. Oh, B.-K. Yu, T. Lee and D.-Y. Kim, *J. Mater. Chem.*, 2009, **19**, 9045.
33 Y.-H. Ha, N. Nikolov, S. K. Pollack, J. Mastrangelo, B. D. Martin and R. Shashidhar, *Adv. Funct. Mater.*, 2004, **14**(6), 615.
34 U. Lang, E. Muller, N. Naujoks and J. Dual, *Adv. Funct. Mater.*, 2009, **19**, 1215.
35 S. Garreau, G. Louarn, J. P. Buisson, G. Froyer and S. Lefrant, *Macromolecules*, 1999, **32**, 6807.
36 S. Garreau, J. L. Duvail and G. Louarn, *Synth. Met.*, 2001, **125**, 325.
37 J. Krajcovic, G. Cik, D. Vegh and F. Sersen, *Synth. Met.*, 1999, **105**, 79.
38 J. Y. Ouyang, C.-W. Chu, F.-C. Chen, Q. F. Xu and Y. Yang, *Adv. Funct. Mater.*, 2005, **15**(2), 203.
39 J. S. Gwag, J. Yi, J. H. Kwon, M. Yoneya and H. Yokoyama, *J. Appl. Polym. Sci.*, 2011, **119**, 325.
40 J. Hoogboom, T. Rasing, A. E. Rowan and R. J. M. Nolte, *J. Mater. Chem.*, 2006, **16**, 1305.